Analytical Methods

Smartphone-based image analysis and chemometric pattern recognition of the thin-layer chromatographic fingerprints of herbal materials

Journal:	*Analytical Methods*
Manuscript ID	AY-ART-12-2018-002698
Article Type:	Paper
Date Submitted by the Author:	11-Dec-2018
Complete List of Authors:	Sibug-Torres, Sarah May; Ateneo de Manila University, Department of Chemistry Padolina, Isagani; Pascual Pharma Corp. Cruz, Philip; Herbanext Laboratories Inc. Garcia, Felan Carlo; Ateneo de Manila University, Department of Electronics, Computer, and Communications Engineering Garrovillas, Mark Joseph; Ateneo de Manila University, Department of Chemistry Yabillo, Maria Regina; Ateneo de Manila University, Department of Chemistry Enriquez, Erwin P.; Ateneo de Manila University, Department of Chemistry

Smartphone-based image analysis and chemometric pattern recognition of the thin-layer chromatographic fingerprints of herbal materials

Sarah May Sibug-Torres[a], Isagani D. Padolina[c], Philip Cruz [d], Felan Carlo Garcia[b], Mark Joseph Garrovillas[a], Maria Regina Yabillo[a], Erwin P. Enriquez[a‡]

[a] Department of Chemistry, Ateneo de Manila University, Katipunan Ave., Loyola Heights, Quezon City, Philippines 1108

[b] Department of Electronics, Computer, and Communications Engineering, Ateneo de Manila University, Katipunan Ave., Loyola Heights, Quezon City, Philippines 1108

[c] Pascual Pharma Corp., 23rd Floor, The Taipan Place, F. Ortigas Jr. Road, Ortigas Center, Brgy. San Antonio, Pasig City, Metro Manila, Philippines 1605

[d] Herbanext Laboratories, Inc., Negros South Road, Bago City, Negros Occidental, Philippines

Corresponding Author
‡epenriquez@ateneo.edu

Abstract

Thin-layer chromatography (TLC) is commonly used as a screening method to verify the identity and quality of dried herbal medicinal plant material. While TLC is relatively simple, the method still requires technical experience and relies on the subjective classification of sample TLC profiles as "within-specifications" or "off-specifications." In this work, we report the development of an objective TLC-based system for the identification and quality assessment of herbal medicinal materials. Our proposed system is a miniaturized Pharmacopeia-based TLC method coupled with a smartphone app that allows for an objective interpretation of TLC profiles via multivariate image analysis and chemometric fingerprinting. An image of the TLC profile is captured using a smartphone camera interfaced with a 3D-printed photo-box, and the analysis is automated using a framework of pre-uploaded algorithms hosted on a cloud server. The TLC profile image is converted to an unfolded red, green, and blue (RGB) channel intensity profile, and classified as "within-specifications" or "off-specifications" using aggregated Soft Independent Modeling of Class Analogy (SIMCA) models. We present the application of our system to two herbal medicinal plants, *Blumea balsamifera* and *Vitex negundo*. The proposed system demonstrates 90.2% sensitivity and 86.2% specificity for *B. balsamifera* classification, and 81.4% sensitivity and 92.0% specificity for *V. negundo* classification when compared to the respective laboratory-based Pharmacopeia TLC protocols for the ability to distinguish authentic samples from non-authentic and degraded samples. The system developed in this work is a cost-effective, rapid method that can serve as an herbal material quality assessment tool in resource-limited settings.

Keywords

thin-layer chromatography, smartphone sensing, pattern recognition, chemometric fingerprinting, image analysis, herbal medicines

Introduction

Traditional herbal medicines have grown in popularity over the past few decades because of their increased integration and acceptance in modern medicine.[1] The increased demand for herbal products has also opened avenues for inclusive growth in the agricultural sector of many developing countries. Since herbal medicinal plants are viewed as high value crops,[2,3] farmers have turned to herbal farming as an alternative livelihood, with many small farms forming community-based cooperatives to supply bulk medicinal plant material to pharmaceutical manufacturers.[4]

However, despite the high demand and interest in herbal farming, manufacturers regularly reject a significant percentage of raw material from suppliers due to quality concerns. Since many herbal medicinal products are only minimally processed into teas and tablets, guaranteeing the safety and quality of these products starts at the raw material.[5] Manufacturers therefore implement strict quality screening before accepting raw material for further processing. Some common grounds for supply rejection include incorrect plant variety, contamination with other plant types, material mishandling or mislabeling, and improper material preprocessing that leads to substandard quality.[6] These rejections result in significant financial losses for the supplier as well as lost opportunity for the manufacturer and marketer. The limited supply of quality raw materials is one of the major factors hindering the growth of the herbal industry in many developing countries.[6]

The loss of raw material early in the supply chain can be attributed to the lack of quality control techniques and technology at the community-based supplier level. Typically, farmers and suppliers do not have access to reliable methods for in-process quality assessment to pre-screen their materials prior to submission to manufacturers. An accessible tool is therefore needed to help mitigate supply rejections as well as to identify key preprocessing steps that may need improvement. An additional challenge, however, is that herbal plant material is usually preprocessed, stored, and pooled in a dried, homogenized form, so distinguishing a plant sample based on its morphological characteristics is no longer feasible at this point. Homogenized plant material, nonetheless, can still be identified based on its chemical profile, which can

be determined by analyzing the sample with techniques such as infrared spectroscopy, Raman spectroscopy, thin-layer chromatography (TLC), or high-performance liquid chromatography (HPLC).[7,8] Most of these methods, however, are too impractical and costly for resource-limited settings.

TLC, however, is the most promising method for adoption in resource-limited settings due to its simplicity and low capital cost. In fact, there are existing TLC-based field test kits in the market such as Speedy TLC Kit[9,10], Global Pharma Health Fund (GPHF)'s MiniLab[11], and Field Forensic Inc.'s microTLC.[12] These kits are based on the TLC analysis of test and standard reference samples, followed by visual comparison of the TLC profiles. The widespread use of these kits demonstrates that with minimal training, TLC can be transferable to non-technical users in resource-limited settings.[13,14] A similar test kit can be developed to assess herbal medicinal materials.

The evaluation of herbal medicinal materials via TLC, however, is not as straightforward as the evaluation of synthetic drugs. While synthetic drugs have known active ingredients and formulations, herbal medicines are complex mixtures of the plant's secondary metabolites, not all of which are known.[15] The analysis of an herbal medicinal plant extract with its standard Pharmacopeia TLC protocol will therefore result in a complex pattern of colored bands, which can be likened to a fingerprint.[16] The profile can be evaluated based on Pharmacopeia acceptance criteria, such as the presence of molecular markers or the matching of the whole sample fingerprint to that of a reference.[8,17] This evaluation, however, can be very subjective and may require significant technical experience in comparing profiles visually. Visual comparison can be challenging because of the inherent variability of plant samples and their TLC profiles due to sourcing from regions with different climatic and soil conditions, processing with different drying methods, or harvesting during different seasons.[7]

A more objective system for evaluating TLC profiles of plant extracts can be achieved using image analysis and chemometric fingerprinting. The image of the TLC fingerprint can be captured using flatbed scanners or charge-coupled device (CCD) cameras, then converted to a multivariate digital signal for chemometric classification. A chemometric classification model is trained based on the fingerprints of

labeled samples, which provide data on the permissible limits of sample variation.[17] The planar chromatography profiles of naturally-derived products such as propolis,[18–21] traditional Chinese medicines,[22–24] spirulina,[25] chamomile tea,[26] and saffron[27] were analyzed in previous studies using multivariate image analysis coupled with principal component analysis (PCA), partial least squares discriminant analysis (PLS-DA), and hierarchical cluster analysis (HCA). These previous studies focused on discriminating samples between different varieties or classifying an authentic sample from known possible adulterants using multi-class classification approaches.

In the context of building a chemometric model for the identification and quality assurance of dried plant material, only the fingerprints of pure, authentic samples can be practically modeled, as possible sample contamination, mislabeling, or degradation can be very open-ended. This problem can be viewed as a novelty detection or one-class classification problem: either an unknown sample is classified as "within-specifications" with respect to the plant species of interest or not ("off-specifications"). A common approach is Soft Independent Modeling of Class Analogy (SIMCA), which models classes independently based on the PCA of the classes of interest.[28] SIMCA has been applied previously for the identification of herbal medicines using HPLC[29,30] and infrared spectroscopy,[31–33] although there have been no previous reports of the approach applied to data from planar chromatography such as TLC.

The image capture and chemometric analysis of TLC profiles is typically conducted using image-capturing devices interfaced with a personal computer, which can be costly and impractical for resource-limited settings. A more practical, cost-effective alternative is a smartphone device. The use of the smartphone platform for field-level and/or resource-limited analysis has been rising in popularity because of its portability, cost-effectiveness, and robust technology including built-in camera and processing power capable of sending and storing data to a cloud server.[34,35] There are recent reports of using a smartphone platform for the TLC image analysis and quantitative determination of single-component pharmaceutical[36,37] and illegal drugs,[38] although there have been no previous reports of a smartphone app for the identification of herbal medicinal materials.

In this work, we aim to develop a method for the pre-screening of herbal medicinal plant materials in resource-limited settings. Our proposed system consists of a miniaturized, Pharmacopeia-based TLC method coupled with smartphone-based multivariate image analysis and SIMCA classification. We demonstrate the application of our system to two widely commercialized herbal medicinal plants in the Philippines[2], *Blumea balsamifera* and *Vitex negundo*, which are used to treat kidney stones[39] and asthma,[40] respectively. We also compare our system to the respective laboratory-based Pharmacopeia TLC protocol for the ability to distinguish authentic samples from non-authentic samples, degraded samples, as well as leaf mixtures. It is our aim that the accessibility of our method will allow community-based suppliers to more effectively manage and pre-screen their materials, potentially reducing rejection rates and improving the supply of quality herbal medicinal raw materials.

Experimental

Reagents

Absolute ethanol was from Chem-Supply; 95% n-hexane was from RCI Labscan Limited, ethyl acetate, 95% H_2SO_4, and vanillin were from Ajax Finechem. Glacial acetic acid was from Macron Fine Chemicals. p-anisaldehyde was from Sigma-Aldrich. *B. balsamifera* standards dihydroquercetin-7,4'-dimethyl ether (DQDE), blumeatin (BL), quercetin (QN), 5,7,3',5'-tetrahydroxyflavanone (THFE), and dihydroquercetin-4'-methyl ether (DQME), and *V. negundo* standard, agnuside (AGN), were from Wuhan ChemFaces Biochemical Co., Ltd. Aluminum TLC silica gel 60 F_{254} plates were from Merck. All reagents used were analytical grade unless otherwise stated.

Collection and preparation of samples

Twenty-two *B. balsamifera* and fifteen *V. negundo* leaf samples were collected from various farms across the Philippines and were authenticated with the Pharmacopeia protocols described in the next subsection. All samples underwent standard primary processing including sorting, washing, drying,

homogenizing, and packing in sealed plastic bags with silica gel desiccants. Different drying methods used to process the samples included oven drying at 60 °C for 4 hours, air drying, and drying via dehydrator. These samples served as within-specifications (WS) samples for the respective plant species.

Off-specifications (OS) samples were artificially prepared by treating pure, WS samples with non-standard processing methods, including treatment with high temperature (oven heating at 100 °C for 2 hours), exposure to high humidity to simulate improper sample storage, fermentation, and incomplete drying followed by sample storage. Various mixtures were also prepared to simulate sample impurity at different weight concentration levels (5, 10, 20, 30, 40, 50, 60, 70, 80, and 90% w/w adulterant). Investigated mixtures included *B. balsamifera* mixed with *Blumea lacera*, and *B. balsamifera* mixed with *V. negundo*.

Analysis of samples with standard Pharmacopeia protocols

All pure *B. balsamifera* and *V. negundo* samples were analyzed with their respective Pharmacopeia protocols summarized in **Table 1**. Analysis was conducted on silica gel 60 TLC plates at a development distance of 10 cm. *B. balsamifera* standards BL, QN, THFE, DQME, and DQDE, and *V. negundo* standard, AGN, were analyzed alongside their respective samples. The prepared OS samples and mixtures were also analyzed to determine if the respective Pharmacopeia protocol and acceptance criteria could correctly distinguish them as "off-specifications."

Adapted TLC method

Simplified, miniaturized versions of the TLC Pharmacopeia protocols for *B. balsamifera* and *V. negundo* were developed as the field TLC kit methods. Sample analysis proceeded as follows. First, approximately 0.1 g of dried homogenized leaf sample was soaked in 1.0 mL 95:5 (v/v) ethanol-water for 30 minutes with occasional shaking. A small amount of the ethanolic extract was decanted into a fresh microtube. Using a calibrated glass capillary tube, 10 μL of the extract was spotted onto a 1.4 cm x 5.2 cm

silica gel 60 TLC plate. Development was performed using a mobile phase of 1:1 (v/v) hexane-ethyl acetate for *B. balsamifera* samples, or 80:10:5 (v/v) ethyl acetate-glacial acetic acid-water for *V. negundo* samples in a 25-mL scintillating vial that served as an improvised developing chamber. After pre-saturating the chamber with 1.0 mL of mobile phase for 5 min, the TLC plate was lowered into the chamber and development proceeded until the solvent reached a pre-marked solvent-front 4.2 mm from the spotting line. The TLC plate was then air dried and dipped in a vanillin-H_2SO_4 solution for *B. balsamifera* samples or anisaldehyde-H_2SO_4 solution for *V. negundo* samples for derivatization. The plate was dried for two minutes and heated for approximately one minute on a custom heater for band visualization. Immediately after visualization, the TLC plate was laminated and fixed onto a plate card using a clear vinyl sticker. All samples were analyzed in triplicate to evaluate method repeatability and subsequent data preprocessing methods.

Image capture with 3D-printed photo-box

To facilitate the image capture of a TLC plate with a smartphone camera, a custom photo-box was designed using AutoCAD 123D Design and 3D-printed using Flashforge Creator Pro 3D printer with acrylonitrile butadiene styrene (ABS) polymer as the printing material. The 3D-printed photo-box was custom designed for the smartphone used in this study, an Asus Zenfone Go 5.0, which was selected because of its relatively low cost (approximately 70 USD) and widespread availability. A slot in the front of the photo-box can hold the smartphone in place so a TLC plate can be photographed at a consistent 10-cm distance from the rear-view camera. Also included in the photo-box was an internal, battery-powered white LED light with diffuser to ensure consistent, uniform lighting conditions for imaging the TLC plate. TLC plates were photographed by sliding the laminated plates through a rear slot in the photo-box. A black mask formed a frame around the TLC profiles to facilitate region-of-interest (ROI) detection during image processing. The black mask also featured a white reference strip (PaperOne All Purpose premium paper) to check for consistent lighting conditions during image capture. The photo-box set-up is shown in **Figure 1**.

Smartphone Application

To objectively classify a sample TLC profile, a smartphone Android application (app) was developed as an interface for image capture, image processing, chemometric analysis, and data storage. A summary of the app work-flow is illustrated in **Figure 2**. The app can be operated as follows. First, the user is required to log-in and select the plant species to be analyzed: *B. balsamifera* or *V. negundo*, which are also listed with their common names in the Philippines, "sambong" and "lagundi", respectively. Afterwards, the user inputs sample details, inserts the TLC plate into the 3D-printed photobox, and captures an image. Images are captured in .JPEG format with a camera resolution of 3 MP (4:3). Once an image is captured, the user is prompted to upload the image to a dedicated cloud server for analysis. If mobile data or wi-fi connection is unavailable, the image is queued for submission until a stable connection is available.

A pre-uploaded algorithm on the cloud server automatically performs all image processing and chemometric analysis with reference profiles and classification models. The image processing steps and the development of the chemometric model are detailed in the next subsections. The user is prompted to repeat image capture if the image is unfocused or if the lighting is not consistent with the lighting of the training images. If all processing is successful, a classification result of "within-specifications" or "off-specifications" is returned to the user. All captured images and results are saved in the app history.

Image analysis and data preprocessing

A custom Python[41] script using SciPy's multi-dimensional image processing package[42] was written to automatically crop, extract, denoise, background correct, and convert TLC profile images to matrices of RGB intensity values. However, prior to analyzing the TLC profiles, initial tests were conducted to determine if lighting conditions during image capture were consistent and uniform based on a white reference strip in the photo-box. To automatically extract the ROIs, images were initially cropped to the approximate location of the TLC profiles. The ROIs from the cropped images were then extracted using a

Gaussian filter mask and bounding box (see *Supplementary Information*, **Figure ESI-1** and **ESI-2** for more details). Extracted TLC profiles were denoised using median filter with a 4-pixel radius, and background corrected using the rolling ball background subtraction algorithm applied separately to each RGB color channel. The rolling background subtraction algorithm was ported to python from the ImageJ[43] Background Subtractor.[44] The images were then converted to a RGB densitograms by obtaining the average intensity horizontally for each of the image's RGB color channels. Per sample, the output was a 750 x 3 matrix, where the first dimension was the spatial dimension of the TLC fingerprint (length), while the second dimension was the intensity component of each RGB channel. Afterwards, the RGB intensity values were inverted by subtracting the intensity values of each color channel from the maximum intensity value of 255.

The RGB matrices of the TLC profiles were ported to R version 3.3.2[45] for further signal preprocessing. To correct variations in signal peak positions, the TLC profiles were aligned with respect to a reference using variable penalty dynamic time warping (VPdtw), implemented with the R VPdtw package version 2.1-11[46]. Alignment of each color channel was performed using a reference-based dilation penalty function and a maximum shift of 100 pixels. Samples that were tested as *B. balsamifera* were aligned with respect to the *B. balsamifera* reference profile (sample ID: BB19), whereas samples tested as *V. negundo* were aligned with respect to the *V. negundo* reference profile (sample ID: VN15). The aligned 750 x 3 matrices were then unfolded into vectors of length 2250. All sample fingerprints were normalized to unit norm prior to modeling.

Chemometric analysis

SIMCA models of the *B. balsamifera* WS class and *V. negundo* WS class were constructed with 95% Q and T^2 Hotelling limits for outliers and single value decomposition method using Multivariate Data Analysis for Chemometrics (mdatools) R package version 0.8.2.[47] Only WS samples were used to train the SIMCA models, while OS samples were used only for validation and testing. Iterated nested k-fold cross-validation (k=5) with 40 iterations was used to tune model parameters and estimate prediction errors. OS

test samples (non-mixtures) were included in the inner cross-validation loop as negative test samples to estimate the specificity or true negative classification rate. The numbers of principal components (PCs) used for the outer cross-validation folds were determined based on the sensitivity (true positive classification rate) and specificity from the corresponding inner cross-validation fold. Model prediction errors were estimated using the sensitivities and specificities from the iterated outer cross-validation loops. Throughout all cross-validation procedures, technical replicate fingerprints were included during modeling to capture uncorrected variations due to sample TLC analysis. Technical replicate fingerprints were always grouped together during the randomized training/testing splits. Samples were mean-centered and scaled relative to the applicable training subset prior to any modeling and testing. The final SIMCA models were pre-uploaded to the smartphone app's dedicated cloud server for future sample classification. The final models were tested with the prepared mixtures to evaluate the capability of the system to detect adulterations.

Results and Discussion

Analysis with TLC Pharmacopeia protocols

The aim of this study was to develop a rapid, objective TLC-based system that can be correlated to the standard Pharmacopeia TLC protocol. Thus, all within-specifications (WS) and prepared off-specifications (OS) samples and mixtures were analyzed initially using the respective Pharmacopeia TLC protocol as the standard test method for comparison. All pure WS samples and prepared OS samples were confirmed as WS and OS, respectively, using the Pharmacopeia acceptance criteria. The TLC profiles of representative *B. balsamifera* and *V. negundo* samples are shown in **Figure 3** (the complete set of TLC profiles and sample details can be found in *Supplementary Information,* **Tables ESI-1** and **ESI-2**). While characteristic patterns are discernible for each plant species, differences in band intensity and the presence or absence of some bands can be sources of uncertainty when visually assessing a sample using the Pharmacopeia acceptance criteria. For example, in some cases, it was unclear whether a certain band

intensity was within an acceptable range. This challenge emphasizes the need for more objective, data-based classification methods especially for users with little or no technical training.

Uncertainty in the Pharmacopeia acceptance criteria was also apparent when laboratory-prepared mixtures were tested. In this study, *B. balsamifera* was mixed with a related plant species, *Blumea lacera.*[48] Also, *B. balsamifera* and *V. negundo* mixtures were prepared to simulate accidental mixing of the two plant samples in a processing center that may be handling both products. Detecting impurities with other plant material is important for herbal medicinal materials, but this can be difficult to achieve using only visual inspection of TLC profiles. Even for trained users, variations in a TLC profile due to the presence of impurities may be mistaken as natural variations in the chemical profiles of the plant materials. We also found that detecting adulteration can be highly dependent on the nature of the adulterating plant material. For example, when *B. balsamifera* was mixed with related species, *B. lacera*, 20% (w/w) impurity was discernible. However, when *B. balsamifera* was mixed with unrelated species, *V. negundo*, only 60% (w/w) impurity was discernible.

It became evident that while some agencies recommend the Pharmacopeia TLC method to assess identity, batch-to-batch uniformity, and purity,[49] the method is not a reliable means to detect impurities. To more effectively detect adulterations using TLC, comprehensive profiling using multiple chromatographic systems can improve the resolution of non-specific adulterants, although this is beyond the scope of this study. These prepared test mixtures were still evaluated using our developed system to determine if improved detection of adulterations can be achieved with the aid of image analysis and chemometric classification.

Analysis of samples with adapted TLC method

To facilitate the transfer of the TLC technique to resource-limited settings, we adapted the Pharmacopeia TLC protocol to a miniaturized set-up with the aim of reducing analysis time and reagent use. A major modification was the abbreviation of the development distance to 4.2 cm, which takes only

5-6 minutes in contrast to the 20-25 minutes needed full development. Additional advantages of this shortened development distance include the use of smaller TLC plates, the miniaturization of the development chamber, shortened chamber saturation times, and the use of lower volumes of organic mobile phase. Although the TLC profiles exhibit band overlap, major bands remain distinguishable just as in the fully-developed TLC profiles (**Figure 3**s).

Another technical challenge in transferring TLC to resource-limited settings is the use of organic solvents. To minimize the use of hazardous organic solvents, ethanol was used instead of methanol in reagent formulations, and extraction was performed with simple soaking and shaking in ethanol for 30 minutes instead of the methanol reflux extraction conducted in the laboratory. However, the organic mobile phases prescribed in the Pharmacopeia protocols were retained in the adapted TLC methods. Although the use of organic solvents can present some usability challenges for a field method, other TLC-based field test kits such as the Speedy TLC Kit[9,10] and GPHF-MiniLab[11] also feature organic solvents as mobile phases. The adoption of these TLC kits in numerous resource-limited settings demonstrates that the use of organic solvents in the TLC method can be transferable to non-technical users with minimal training in proper handling techniques and precautions.[13,14]

We also included additional steps in the TLC protocol to minimize method-related variations. A step in the operation of the TLC that is prone to error is the band visualization of the TLC plate. The color and intensity of the bands tend to fade very quickly, so to minimize error, we included a step where the TLC plate is laminated with a clear vinyl sticker immediately after band visualization. This step helps retain the color of the fingerprint for as long as 30 minutes, which is more than enough time for image capture.

Other possible sources of error that can result in TLC profiles with variable band intensities include insufficient extraction, sample application, and derivatization. These errors can be minimized with careful adherence to the instructions provided in the TLC kit.

TLC plate imaging

For smartphone-based imaging, lighting can be a major source of variation that can affect the quality of the images used for chemometric analysis. In the early development of our system, we evaluated the use of various light sources, including natural daylight, and fluorescent and LED lamps. Finally, however, to ensure that the lighting conditions are consistent and reproducible in different settings, we designed a 3D-printed photo-box with a built-in, battery-powered LED light for the image capture of TLC profiles. To further ensure consistent lighting conditions, a white reference strip was also built into the photo-box. All images captured using the photo-box were checked for the mean RGB intensity values of this white reference strip. In all training set images, the mean RGB intensity values of the reference strip are R = 166.0 (standard deviation, s.d. 0.3), G = 166.1 (s.d. 0.3), and B = 166.1 (s.d. 0.3). These values are used as lighting calibration checks prior to further image processing: if the color of the white reference strip is beyond the acceptable range, the user will be prompted to repeat image capture or to troubleshoot. Failed calibration checks may occur if flash is accidentally enabled during image capture (**Figure ESI-2**), if the battery is failing, or if the white reference strip is blemished somehow.

Image analysis and preprocessing of fingerprints

Image analysis of the TLC profile was conducted to pre-process and convert the profile image into a digital fingerprint that can be used as input variables for multivariate analysis. We automated all image analysis and chemometric preprocessing using pre-uploaded algorithms on a dedicated cloud server, which receives the sample image via the smartphone app. The overall schematic for the preprocessing of a sample TLC image is illustrated in **Figure 4**.

Conversion to unfolded RGB intensity profiles. The TLC profiles from the adapted method feature several overlapping bands that are difficult to distinguish using only greyscale intensity values. Thus, we retained the color information contained in the TLC profile by obtaining intensity profiles for each RGB color channel. Color can be used to distinguish between components with similar retention factors, which

is especially important in cases where bands are not completely resolved. Other groups studying the TLC fingerprints of natural products have also retained color information using this strategy,[18–20,26] although not all groups have opted to use all three channels. Hemmateenejad *et al*. noted that chromatograms with overlapping, colored bands are best characterized with all three color channels.[50] We therefore opted to use all three color channels as input variables for classification, yielding a three-way data set (IxJxK) wherein a matrix of JxK (J number of intensity values for K color channels) is measured for I samples. Chemometric techniques, however, are often suited for two-way data.[51] A strategy for adapting three-way data for two-way chemometric analysis is through unfolding, wherein the data is converted to a two-way data matrix, (I x (JxK)) by appending the three intensity profiles one after the other. One disadvantage of this approach is that the relationship between the color channels is lost. Nevertheless, multivariate analysis can still be performed satisfactorily on unfolded data sets compared to more complex three-way data analysis.[50]

Profile alignment. An important preprocessing step for our application is profile alignment, which corrects band shifts that occur due to non-controllable variable conditions such as temperature, humidity, or slight changes in mobile phase solvent composition. These factors are especially difficult to control when TLC is performed outside a laboratory setting. Alignment corrects these shifts by adjusting the positions of the bands to match those of a reference, thereby ensuring that the variation in the fingerprints is primarily due to chemical composition and not due to external factors.

To align the TLC profiles with minimal signal distortion, we implemented variable penalty dynamic time warping (VPdtw) algorithm. VPdtw limits the possible shifts for alignment by using a penalty function, which is calculated from the peaks of the reference profile. The requirement for peaks for the implementation of VPdtw necessitates color inversion of the TLC profiles. The RGB color system is an additive system in which the color white has RGB intensity values of (255, 255, 255), whereas black has RGB values of (0,0,0). Inverting the colors of an image involves subtracting each RGB value from 255, the maximum intensity value. The original TLC profiles have light backgrounds where bands appear as valleys, so when inversion is performed, the bands are transformed to peaks. Step (6) in **Figure 4** shows an inverted

sample profile overlaid with a reference profile before and after alignment. The unaligned profile shows significant variation in the position of the sample peaks relative to the reference, but after implementation of VPdtw, the band positions are matched, even when the sample profile has different band intensities compared to the reference.

Overall, the preprocessing steps correct some of the variations in the TLC profiles due to external factors. **Figure 5** shows the technical replicates of sample BB21 before and after all preprocessing steps. The original TLC profile images show slight variations in band position and overall intensity, but many of these variations are corrected after preprocessing. The PCA scores plots of the *B. balsamifera* and *V. negundo* WS samples (with OS samples projected onto the WS class principal component model) in **Figure 6** show that WS technical replicates as well as the entire WS sample set become grouped more closely together after preprocessing. It must be noted, however, that the preprocessing procedures were unable to correct for slight variations in band intensity, which could be due to the extraction and derivatization steps in the TLC method. For the chemometric analysis, technical replicate samples were included in the modeling stage so that these uncorrected variations are also built into the model.

Chemometric analysis

Since our objective is to assess a sample as either acceptable (WS) or not (OS) for a given herbal plant, we opted to use a novelty detection approach in which we model only the TLC profiles of WS samples. SIMCA was selected as it is based on class PCAs, which is useful in this case since it can reduce the dimensionality of the input TLC profile vectors.

Model tuning. Sensitivity and specificity rates were used as classification performance metrics to optimize each SIMCA model for the number of principal components (PCs) to be retained. Ideally, both high sensitivity and specificity rates are desirable. However, tuning often involves a trade-off between these two metrics, so it becomes necessary to assess the practical implications of two types of classification errors: false negatives and false positives. For our application, the kit is a pre-screening tool for community-based

suppliers to assess the quality of their materials before submitting them to pharmaceutical manufacturers. A false negative is undesirable since it may lead to the decision to stall the submission of acceptable material, resulting in lost economic opportunity for the farmer and supplier. However, a false positive can result in even greater economic loss, as it may lead to the decision to submit material that is actually off-specifications. Since this material will be tested again when received at the manufacturing facility, it is likely that it will be rejected, resulting in wasted transportation costs for the supplier as well as possible loss of credibility. Therefore, an optimal specificity (lower false positive rate) was prioritized when selecting the number of PCs to be retained during the tuning stage.

To tune the SIMCA models and to estimate the classification performances, we used an iterated nested 5-fold cross-validation strategy. The sample sizes used in this study are currently limited (n=22 for WS *B. balsamifera* class, and n=15 for WS *V. negundo* class) compared to the sample sizes recommended for building classification models, so the typical hold-out strategy for training, validation, and testing can result in unreliable performance estimates due to model instability.[52] The nested k-fold cross-validation strategy aims to maximize small sample sizes for training, validation, and testing to improve model performance estimates. An illustrative schematic of the nested cross-validation procedure used in this study is shown in the *Supplementary Information,* **Figure ESI-3**. It should also be noted that only WS samples were used for training the model, while OS samples were included in the nested cross-validation procedure as validation or test samples to estimate the specificity rate of the models. The inclusion of negative samples in validating and testing one-class classification models was recommended by Zhuang *et al.* in order to avoid overfitting the model towards the target class.[53]

The nested k-fold cross-validation procedure was repeated using new random splits for each iteration to evaluate model stability. Model stability can be first evaluated during the inner cross-validation loops: stable models will ideally yield the same optimized model hyperparameters (number of PCs retained), and similar validation sensitivity and specificity rates across iterations.[52] For both *B. balsamifera* and *V. negundo* SIMCA model tuning, the inner cross-validation models were observed to be unstable most

likely due to the small sample sizes used (**Tables ESI-3** and **ESI-4**). For WS *B. balsamifera* SIMCA modelling, tuning during the inner cross-validation loops resulted in varying number of PCs retained (1-4 PCs). Similarly, for WS *V. negundo* SIMCA modelling, tuning resulted in 1-2 PCs retained.

Model aggregation. Since we observed model instability during iterated nested k-fold cross-validation, the predictions of the individual outer cross-validation models were aggregated to yield a final model for future prediction applications. Model aggregation is a strategy in which the predictions of different models are combined; in the case of classification models, aggregation can be done with a majority vote of the model predictions.[52] In our case, aggregation of the outer cross-validation models was performed by majority 2/3 vote. Most cases yielded consistent classifications across the individual models, and thus readily obtained the required 2/3 majority vote to be classified as either WS or OS. On the other hand, there were cases in which the individual predictions for a sample were inconsistent, therefore failing to obtain a majority 2/3 vote. In these cases, the algorithm will abstain, and a classification will not be assigned to minimize the risk of misclassification.

The final sensitivity and selectivity rates obtained for the aggregated SIMCA models were 90.2% sensitivity and 86.2% specificity for *B. balsamifera*, and 81.4% sensitivity and 92.0% specificity for *V. negundo*. Although the aggregated model strategy now requires a sample to be tested with multiple models, this strategy can nevertheless minimize the uncertainty of predictions from classification models built with a limited number of training samples. However, there were still some consistent sample misclassifications (**Figures ESI-4** and **ESI-5**), such as samples BB22 (WS sample misclassified as OS) and BB_OS2 (OS sample misclassified as WS) for the *B. balsamifera* model, and sample VN02 (WS sample misclassified as OS) for the *V. negundo* model. The TLC profiles of the misclassified WS samples appear to have band intensities that are on the upper extremes relative to the profiles of the entire WS training set. Likewise, OS samples which were misclassified as WS appear to have TLC profiles with most of the characteristic features of the WS training set profiles, but with just some features that are slightly faded (**Figure 3**). Incorporation of additional training samples that augment the representation of these "borderline" cases

may minimize these misclassifications. We anticipate the improvement in the reliability of the classification models upon the incorporation of additional training samples in the future.

The proposed system was also applied to the laboratory-prepared mixtures in order to evaluate the capability of the system to detect adulterations. However, similar to the standard Pharmacopeia method, the SIMCA classification models had varying performances based on the nature of the adulterant plant. The *V. negundo* model showed significant improvement as it can detect 20% (w/w) contamination with *B. balsamifera*. On the other hand, for adulterated *B. balsamifera* samples, the system demonstrated comparable performance to that of the conventional Pharmacopeia protocol: the *B. balsamifera* model can only detect at least 30% (w/w) contamination with *B. lacera* and 70% (w/w) contamination with *V. negundo*. Further modification of the TLC system can be explored in future studies to improve the capability of the system to detect adulterations with other plant material.

Nevertheless, it should be noted that similar classification performance as the conventional Pharmacopeia protocol is achievable using abbreviated TLC profiles coupled with the image analysis and chemometric fingerprinting (sensitivity and specificity values greater than 80%). In contrast, the same classification performance will be difficult by visual inspection alone. Furthermore, the TLC-based system will provide community-based suppliers a field-ready prescreening tool for herbal medicinal materials, which should result in lower rejection rates as well as a means for them to improve their postharvest preprocessing.

Conclusions

A miniaturized, Pharmacopeia-based TLC method and smartphone app were developed to assess the identity and quality of dried herbal medicinal leaf material. A plant sample can be assessed by analyzing its extract using a simplified TLC method and capturing an image of the TLC profile using a smartphone app and a 3D-printed photo-box. The smartphone app then sends the image to a dedicated cloud server with pre-uploaded algorithms that automate the multivariate image analysis and chemometric fingerprinting using aggregated SIMCA models for the plant species of interest. To our knowledge, our system is the first reported use of a smartphone app for the pattern recognition of TLC profiles. Avenues for future system development include the incorporation of additional training samples to improve classification performance and modification of the TLC solvent systems to improve adulteration detection and to improve ease-of-use.

While the use of the smartphone app greatly improves the user-friendliness of the TLC profile interpretation, the method is still based on TLC, which may present some challenges when the system is transferred to users with minimal technical background. A balance between practicality on the field and technical reliability was explored continuously. Additional steps in the method and the chemometric preprocessing were therefore included to help mitigate sources of variation in the TLC method that can affect the generation of a reliable sample fingerprint for chemometric classification. Thus, the TLC method was adapted to be relatively simple with the potential for transfer to users with minimal training.

Overall, the system developed in this work is a cost-effective, rapid method that can serve as a potential prescreening tool for verifying the identity and quality of herbal medicinal materials in resource-limited settings. Although we developed the method with the herbal supply chain in mind, the application of the method can be expanded to assess the freshness and/or authenticity of herbal medicinal finished products or food products. The accessibility of the method can lead to improved quality assessment from raw materials to finished products.

Conflicts of interest

There are no conflicts of interest to declare.

Acknowledgements

The authors thank USAID-STRIDE (Carwin Grant No. 0213997-G-2015-00) for the financial support, Rogomi, Inc. for the mobile app interface development, and Glued Creative Technologies, Inc. for the cloud server and database development. We also acknowledge Dr. Rene Macahig and Mr. Kevin Jace Miranda for the helpful initial discussions. We are especially grateful to the various farms, processing plants, and local government units that assisted us in acquiring some of the samples used in the study, as well as providing invaluable end-user feedback on the test kit developed in this study.

References

1 M. Ekor, *Front. Pharmacol.*, 2014, **4**, 1–10.
2 A. S. Jose, *Financial Viability of Medicinal Plant Farming*, 2003, vol. 15.
3 H. Sher, A. Aldosari, A. Ali and H. J. de Boer, *J. Ethnobiol. Ethnomed.*, 2014, **10**, 1–16.
4 A. Z. M. M. Rashid, H. Tunon, N. A. Khan and S. A. Mukul, *Eur. J. Environ. Sci.*, 2014, **4**, 60–68.
5 S. Govindaraghavan, *J. Diet. Suppl.*, 2008, **5**, 176–212.
6 V. M. Shinde, K. Dhalwal, M. Potdar and K. R. Mahadik, *Int. J. Phytomedicine*, 2009, **1**, 4–8.
7 S. Govindaraghavan, J. R. Hennell and N. J. Sucher, *Fitoterapia*, 2012, **83**, 979–988.
8 J. Sendker and H. Sheridan, in *Toxicology of Herbal Products*, eds. O. Pelkonen, P. Duez, P. M. Vuorela and H. Vuorela, Springer International Publishing, Cham, 2017, pp. 29–65.
9 A. S. Kenyon, P. E. Flinn and T. P. Layloff, *J. AOAC Int.*, 1995, **78**, 41–49.
10 J. Sherma, *Acta Chromatogr.*, 2007, **19**, 5–20.
11 R. W. O. Jähnke, *Pharm. Ind.*, 2004, **66**, 1187–1193.
12 Field Forensics: microTLC™ Field Analysis of Explosives and Drugs, https://www.fieldforensics.com/microtlc-rapid-pre-screen-presumptive-id/, (accessed 3 December 2018).
13 A. Petersen, N. Held and L. Heide, *PLoS One*, 2017, **12**, e0184165.
14 F. Khuluza, S. Kigera, R. W. O. Jähnke and L. Heide, *Malar. J.*, 2016, **15**, 1–7.
15 Y.-Z. Liang, P. Xie and K. Chan, *J. Chromatogr. B*, 2004, **812**, 53–70.
16 G. Alaerts, B. Dejaegher, J. Smeyers-verbeke and Y. Vander Heyden, 2010, 900–922.
17 C. Tistaert, B. Dejaegher and Y. Vander Heyden, *Anal. Chim. Acta*, 2011, **690**, 148–161.
18 P. Ristivojević, F. L. Andrić, J. Đ. Trifković, I. Vovk, L. Ž. Stanisavljević, Ž. L. Tešić and D. M. Milojković-Opsenica, *J. Chemom.*, 2014, **28**, 301–310.
19 C. Sârbu and A. C. Moţ, *Talanta*, 2011, **85**, 1112–1117.
20 T. X. Tang, W. Y. Guo, Y. Xu, S. M. Zhang, X. J. Xu, D. M. Wang, Z. M. Zhao, L. P. Zhu and D. P. Yang, *Phytochem. Anal.*, 2014, **25**, 266–272.
21 D. Fichou, P. Ristivojević and G. E. Morlock, *Anal. Chem.*, 2016, **88**, 12494–12501.
22 R. Tian, P. Xie and H. Liu, *J. Chromatogr. A*, 2009, **1216**, 2150–2155.
23 X. P. Cheng, H. M. Cai, P. He, Y. Zhang and R. T. Tian, *Anal. Methods*, 2013, **5**, 6325–6330.
24 K. H. Wong, V. Razmovski-Naumovski, K. M. Li, G. Q. Li and K. Chan, *J. Pharm. Biomed. Anal.*, 2014, **95**, 11–19.
25 P. K. Zarzycki, M. B. Zarzycka, V. L. Clifton, J. Adamski and B. K. Głód, *J. Chromatogr. A*, 2011, **1218**, 5694–5704.
26 E. Guzelmeric, P. Ristivojević, I. Vovk, D. Milojković-Opsenica and E. Yesilada, *J. Pharm. Biomed. Anal.*, 2017, **132**, 35–45.
27 H. Sereshti, Z. Poursorkh, G. Aliakbarzadeh and S. Zarre, *Food Control*, 2018, **90**, 48–57.
28 R. G. Brereton, in *Chemometrics for Pattern Recognition*, John Wiley & Sons, Ltd, Chichester, UK, 2009, pp. 233–287.
29 J. R. Lucio-Gutiérrez, J. Coello and S. Maspoch, *Anal. Chim. Acta*, 2012, **710**, 40–49.
30 E. Deconinck, C. A. S. Djiogo and P. Courselle, *J. Pharm. Biomed. Anal.*, 2017, **143**, 48–55.
31 J. R. Lucio-Gutiérrez, J. Coello and S. Maspoch, *Food Res. Int.*, 2011, **44**, 557–565.
32 E. Deconinck, C. De Leersnijder, D. Custers, P. Courselle and J. O. De Beer, *Anal. Bioanal. Chem.*, 2013, **405**, 2341–2352.
33 I. C. Yang, C. Y. Tsai, K. W. Hsieh, C. W. Yang, F. Ouyang, Y. M. Lo and S. Chen, *J. Food Drug Anal.*, 2013, **21**, 268–278.
34 K. E. McCracken and J.-Y. Yoon, *Anal. Methods*, 2016, **8**, 6591–6601.
35 X. Huang, D. Xu, J. Chen, J. Liu, Y. Li, J. Song, X. Ma and J. Guo, *Analyst*, 2018, **143**, 5339–5351.
36 H. Yu, H. M. Le, E. Kaale, K. D. Long, T. Layloff, S. S. Lumetta and B. T. Cunningham, *J. Pharm.*

Biomed. Anal., 2016, **125**, 85–93.
37 A. Shahvar, M. Saraji and D. Shamsaei, *Sensors Actuators, B Chem.*, 2018, **255**, 891–894.
38 F. Tosato, T. R. Rosa, C. L. M. Morais, A. O. Maldaner, R. S. Ortiz, P. R. Filgueiras, K. M. Gomes Lima and W. Romão, *Anal. Methods*, 2016, **8**, 7632–7637.
39 Y. Pang, D. Wang, Z. Fan, X. Chen, F. Yu, X. Hu, K. Wang and L. Yuan, *Molecules*, 2014, **19**, 9453–9477.
40 A. S. Vishwanathan and R. Basavaraju, *eJournal Biol. Sci.*, 2010, **3**, 30–42.
41 K. J. Millman and M. Aivazis, *Comput. Sci. Eng.*, 2011, **13**, 9–12.
42 E. Jones, E. Oliphant and P. Peterson, SciPy: Open Source Scientific Tools for Python, http://www.scipy.org/, (accessed 15 February 2018).
43 C. A. Schneider, W. S. Rasband and K. W. Eliceiri, *Nat. Methods*, 2012.
44 M. Balatsko, *GitHub*, 2018.
45 R Foundation for Statistical Computing, 2016.
46 D. Clifford and G. Stone, *J. Stat. Softw.*, 2012, **47**, 1–17.
47 A. Sergey, K. Maintainer and S. Kucheryavskiy, 2017, 178.
48 P. Pornpongrungrueng, F. Borchsenius, M. Englund, A. A. Anderberg and M. H. G. Gustafsson, *Plant Syst. Evol.*, 2007, **269**, 223–243.
49 *Guidelines on the Registration of Herbal Medicines*, Republic of the Philippines, 2004.
50 B. Hemmateenejad, N. Mobaraki, F. Shakerizadeh-Shirazi and R. Miri, *Analyst*, 2010, **135**, 1747–58.
51 A. C. Olivieri and G. M. Escandar, *Pract. Three-w. Calibration*, 2014, 27–45.
52 C. Beleites and R. Salzer, *Anal. Bioanal. Chem.*, 2008, **390**, 1261–71.
53 L. Zhuang and H. Dai, *J. Comput.*, 2006, **1**, 32–40.
54 *Philippine Pharmacopeia 1*, Department of Health - Bureau of Food and Drugs, Muntinlupa, Philippines, 2004.
55 US Pharmacopeial Convention, Vitex negundo Leaf, https://hmc.usp.org/monographs/vitex-negundo-leaf-1-1.

Tables

Table 1. Pharmacopeia protocols for *B. balsamifera* and *V. negundo*

	B. balsamifera	*V. negundo*
Reference	Philippine Pharmacopeia[54]	US Pharmacopeia[55]
Extraction	1 g leaf sample with 10 mL 95% (v/v) ethanol, soak for 30 minutes	2 g leaf sample with 25 mL methanol, 10-minute reflux
Sample Volume	10 µL	10 µL
Mobile Phase	1:1 (v/v) hexane : ethyl acetate	80:10:5 (v/v) ethyl acetate : glacial acetic acid : water
Visualization reagent	Vanillin- H_2SO_4 (prepared with 1:1 (v/v) 1% vanillin in 95% ethanol, 10% H_2SO_4 in 95% ethanol)	Anisaldehyde-H_2SO_4 (prepared with 170 mL methanol, 20 mL glacial acetic acid, 10 mL H_2SO_4 and 1 mL p-anisaldehyde)
Acceptance Criteria	Profile matches that of reference profile under visible light, UV 254 nm, 366 nm, and vanillin derivatization	The presence of the following bands with increasing R_f value: "*two weak grey-brown, one pink, one dark-brown, one strong pink, and one pink*"[55]

Table 2. Inner and outer cross-validation, and aggregated model parameters for *B. balsamifera* and *V. negundo* SIMCA models from iterated nested 5-fold cross-validation (CV)

		***B. balsamifera* SIMCA models**	***V. negundo* SIMCA models**
Inner CV Parameters	Number of components	1-4	1-2, 4
	% Cumulative Variance	1 component: 20.7% (s.d. 1.0%) 2 components: 38.1% (s.d. 2.1%) 3 components: 47.7% (s.d. 2.1%) 4 components: 55.4% (s.d. 0.7%)	1 component: 22.83% (s.d. 1.9%) 2 components: 33.6% (s.d. 1.7%) 4 components: 53.9% (s.d. 0.3%)
	Sensitivity	87.9% (s.d. 5.1%)	71.4% (s.d. 7.1%)
	Specificity	90.8% (s.d. 6.1%)	93.9% (s.d. 5.3%)
Outer CV Parameters	Sensitivity	87.1% (s.d 4.0%)	76.9% (s.d. 4.6%)
	Specificity	86.3% (s.d. 3.6%)	90.5% (s.d. 4.0%)
Aggregated Model Parameters	Sensitivity	90.2%	81.4%
	Specificity	86.2%	92.0%
	Classification of mixtures	5-20% (w/w) *B. lacera* misclassified 5-60% (w/w) *V. negundo* misclassified	5-10% (w/w) *B. balsamifera* misclassified

Figures

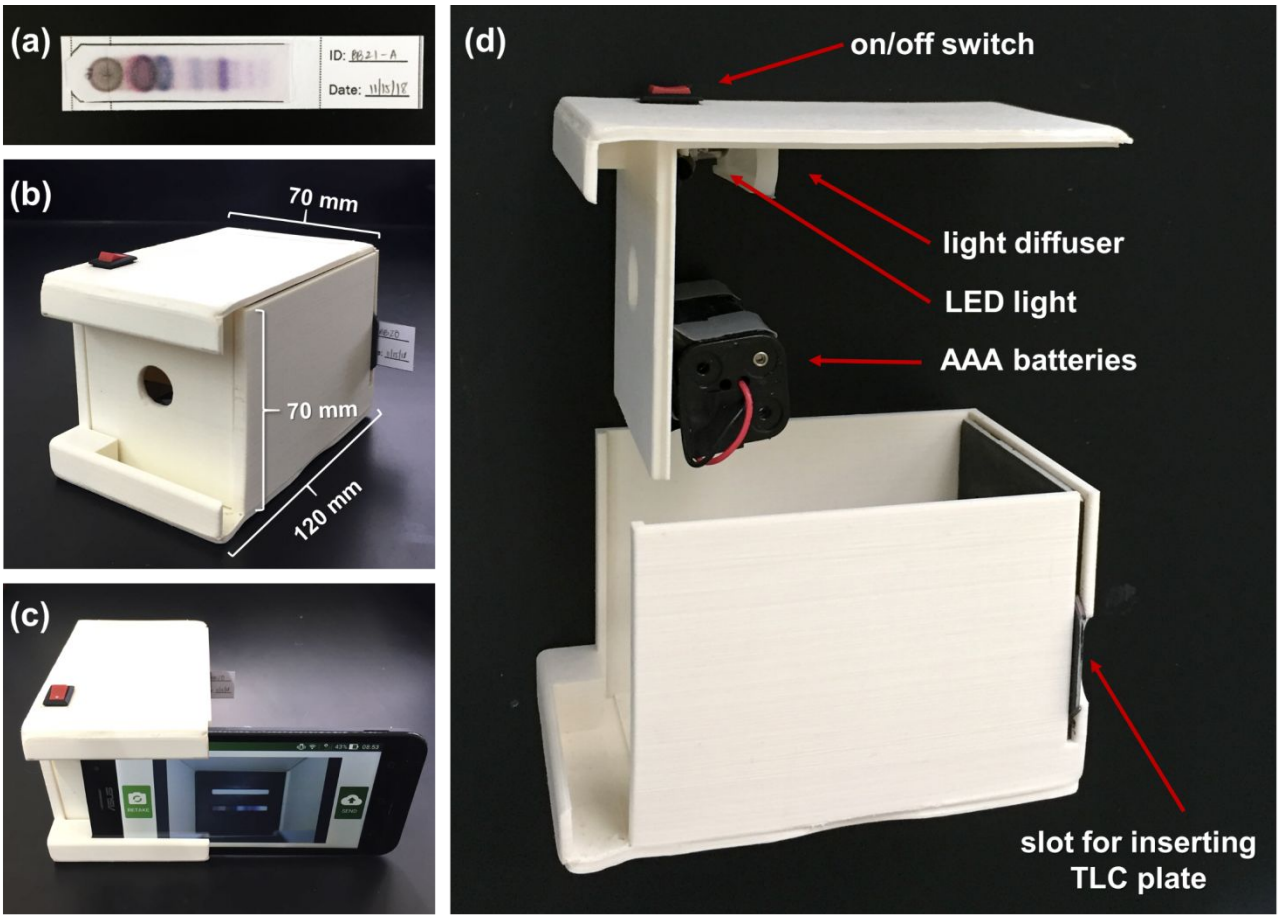

Figure 1. System for smartphone TLC plate imaging. (a) A developed TLC plate is mounted and laminated on a plate card, then inserted into (b) the custom 3D-printed photo-box with internal light source. (c) The smartphone, an Asus Zenfone Go 5.0, is inserted into front slot of the photo-box for TLC plate imaging. Internal components of photo-box are shown in (d).

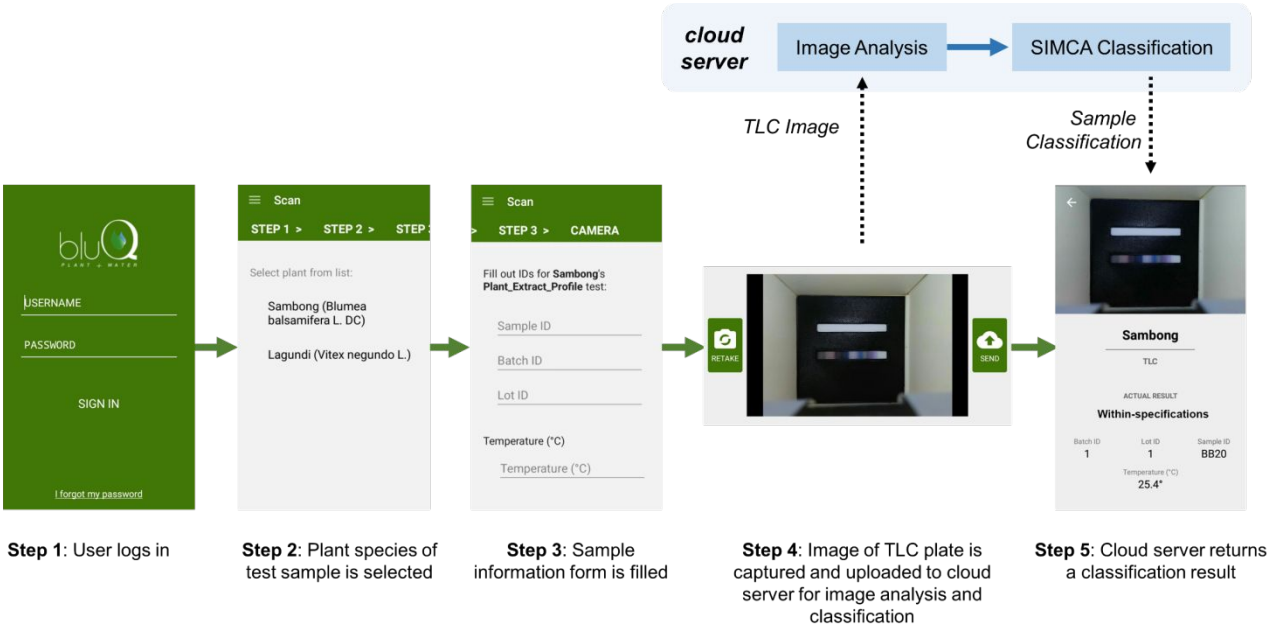

Step 1: User logs in

Step 2: Plant species of test sample is selected

Step 3: Sample information form is filled

Step 4: Image of TLC plate is captured and uploaded to cloud server for image analysis and classification

Step 5: Cloud server returns a classification result

Figure 2. Screenshots demonstrating the "bluQ – PlantQ" app workflow

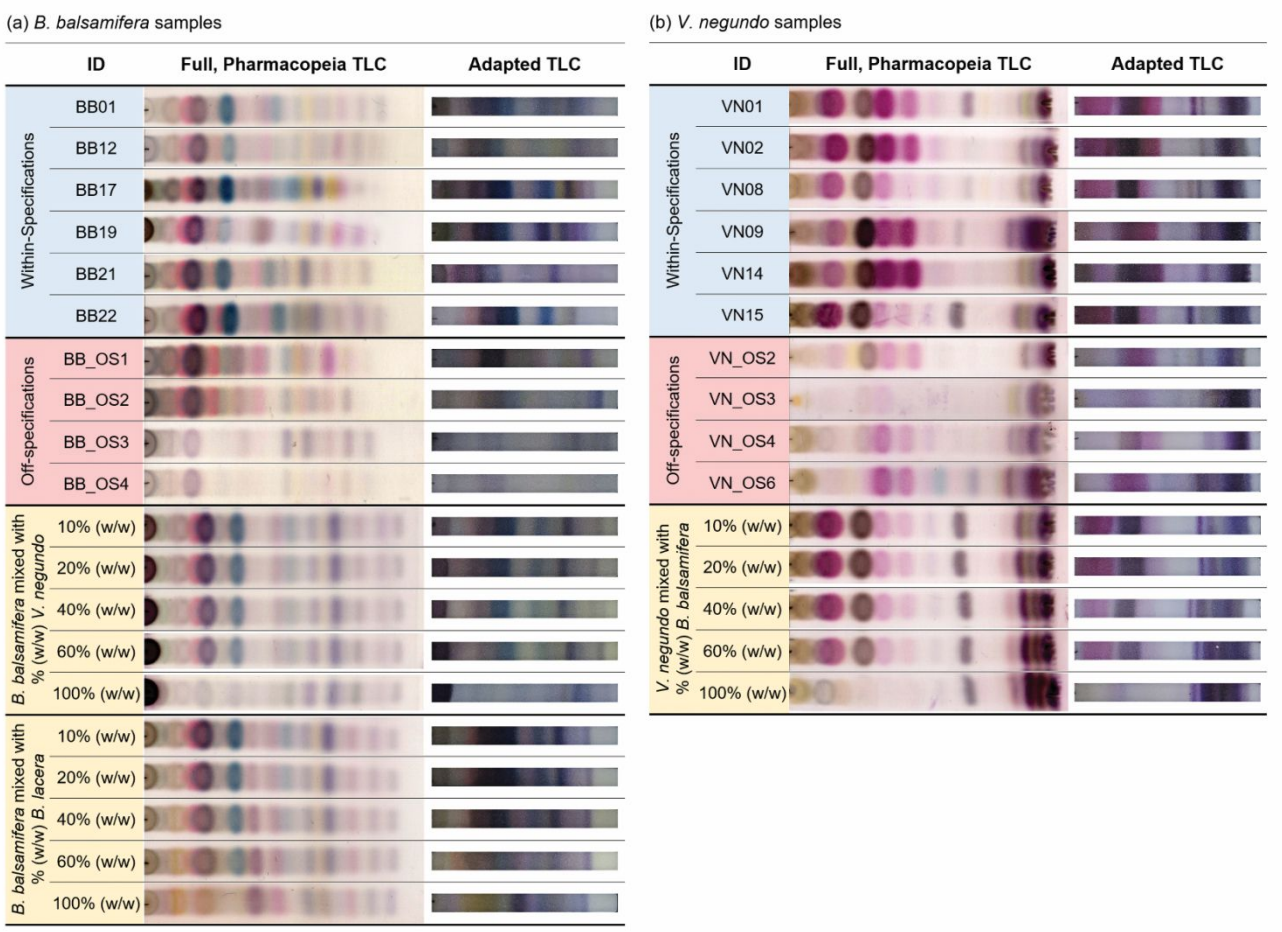

Figure 3. Representative profiles of (a) *B. balsamifera* and (b) *V. negundo* samples analyzed using the standard Pharmacopeia TLC protocol, and the adapted TLC method.

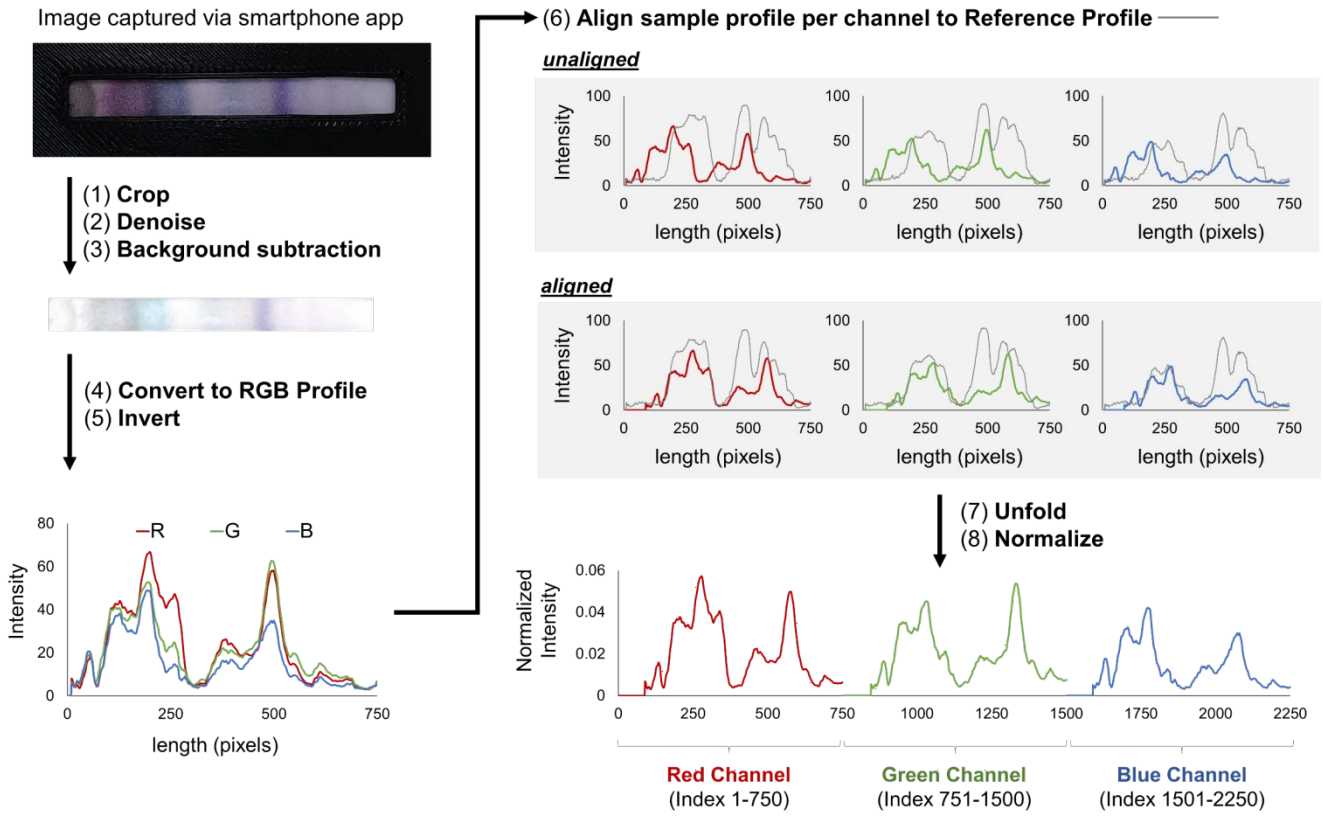

Figure 4. Schematic for image analysis and chemometric preprocessing steps

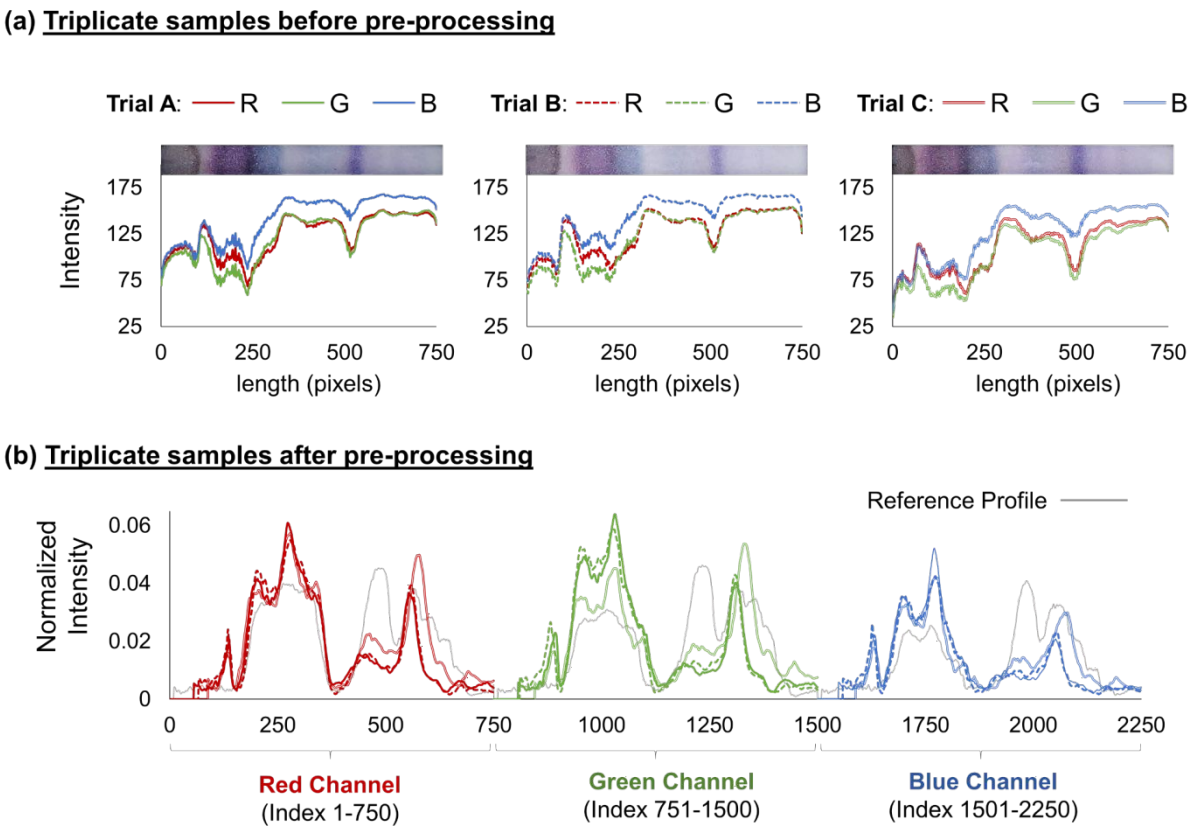

Figure 5. The RGB intensity profiles of sample BB21 technical replicates A, B, and C (a) before preprocessing and (b) after preprocessing.

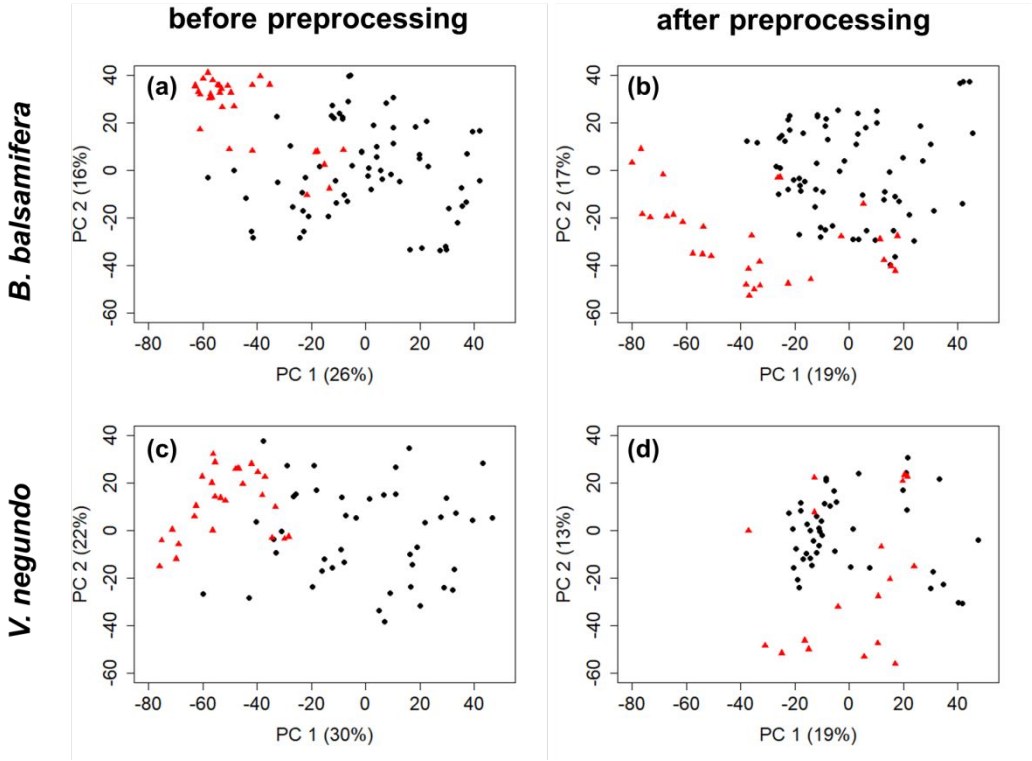

Figure 6. PCA scores plots of *B. balsamifera* WS samples with projected OS samples (a) before and (b) after preprocessing, and *V. negundo* WS samples with projected OS samples (c) before and (d) after preprocessing. (● = WS samples, ▲ = OS samples)

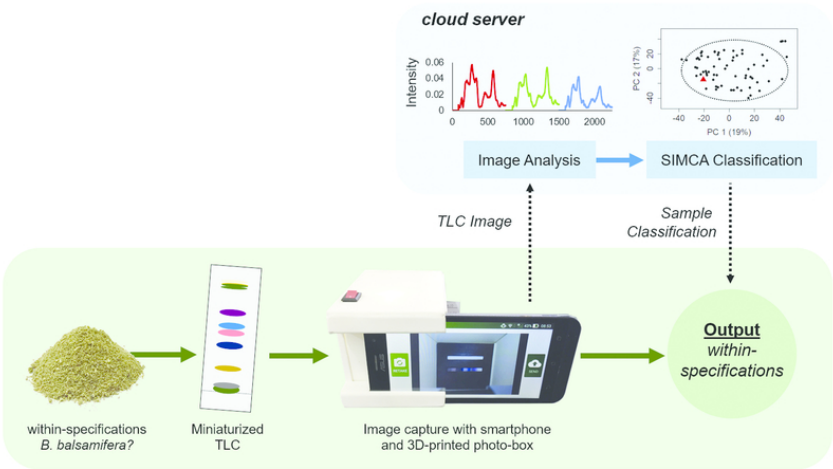

A Pharmacopeia-based TLC method was coupled with a smartphone app for the in-field screening of herbal medicinal materials.

79x39mm (300 x 300 DPI)